Contribution from the Research Laboratory for Nuclear Reactors,
Tokyo Institute of Technology, O-okayama, Meguro-ku, Tokyo 152, Japan

Nuclear Magnetic Resonance Study of the Kinetics of Ligand-Exchange Reactions in Uranyl Complexes. 5. Exchange Reaction of Acetylacetonate in Bis(acetylacetonato)(dimethyl sulfoxide)dioxouranium(VI)

YASUHISA IKEDA, HIROSHI TOMIYASU, and HIROSHI FUKUTOMI*

Received November 18, 1983

The kinetics of the exchange reaction of acac in $UO_2(acac)_2Me_2SO$ (acac = acetylacetonate, Me_2SO = dimethyl sulfoxide) has been studied in o-$C_6H_4Cl_2$ by means of ^1H NMR. The exchange rate depends on the concentration of the enol isomer of acetylacetone in its low region and approaches to the limiting value in its high region. The rate-determining step seems to be ring opening for one of two coordinated acac ions. The kinetic parameters of this step are as follows: $k(25\ °C) = 2.04\ s^{-1}$, $\Delta H^* = 66.4 \pm 8.4$ kJ mol^{-1}, and $\Delta S^* = -17.1 \pm 26.8$ J K^{-1} mol^{-1}. It was found that the exchange rate is decreased by addition of free Me_2SO. This is explained by considering the competition of Me_2SO with the enol isomer in attacking the four-coordinated intermediate in the equatorial plane or the outer-sphere complex formation between $UO_2(acac)_2Me_2SO$ and free Me_2SO.

In spite of a large number of studies of ligand-exchange reactions for uranyl complexes with unidentate ligands,[1-10] only limited information is available concerning the corresponding reactions in uranyl complexes with bidentate ligands such as β-diketonate.[11,12]

In our earlier papers,[13,14] we reported kinetic studies for the uranyl β-diketonato complexes, i.e. the Me_2SO exchange reaction in $UO_2(acac)_2Me_2SO$ and the intramolecular exchange reactions of methyl groups of acac in $UO_2(acac)_2L$ (L = Me_2SO, *N*,*N*-dimethylformamide (dmf), and *N*,*N*-diethylformamide (def)). In the course of these kinetic studies, it was found that the exchange rate of acac between the inner and outer spheres of $UO_2(acac)_2L$ was much slower than that of the above two reactions. This paper deals with the kinetics and mechanism of the exchange of acac in $UO_2(acac)_2Me_2SO$.

Experimental Section

Materials. The $UO_2(acac)_2Me_2SO$ complex was synthesized by the same method as described in a previous paper.[13] Acetylacetone (Hacac) (Wako Pure Chemical Ind. Ltd.) was stored over K_2CO_3 and distilled twice in vacuo. *o*-Dichlorobenzene was distilled twice in vacuo and stored over 3A molecular sieves.

Measurements of the NMR, UV, and IR Spectra. ^1H NMR spectra were measured by using a JEOL JNM-MH-100 NMR spectrometer equipped with a JNM-VT-3B temperature controller. Ultraviolet and infrared spectra of $UO_2(acac)_2Me_2SO$ in o-$C_6H_4Cl_2$ and of $UO_2(acac)_2Me_2SO$ in o-$C_6H_4Cl_2$ containing free Hacac were measured by using a JASCO UVIDEC-505 spectrophotometer and a JASCO DS-701G IR spectrophotometer, respectively. The samples for the ^1H NMR measurements were prepared by the same method as described previously.[13] The water concentrations included in samples were measured by using a Mitsubishi Chemical Ind. Ltd. CA-02 Karl-Fischer titrator. The maximum concentration of water was kept at less than 5.5×10^{-3} M (M = mol dm^{-3}).

Measurements of the Keto–Enol Equilibrium Constant for Acetylacetone. Acetylacetone is in tautometric equilibrium between the enol and keto forms. The fractions of the enol and keto forms of Hacac in o-$C_6H_4Cl_2$ were measured from the areas of the methyl proton signals of the enol and keto isomers. The fraction measurements were made in o-$C_6H_4Cl_2$ containing 0.131 and 1.0 M Hacac at various temperatures ranging from 40 to 140 °C. The equilibrium constant, K = [keto]/[enol], where [keto] and [enol] denote the concentrations of the keto and enol isomers of Hacac, respectively, was calculated from the fractions. Figure 1 shows the plot of $-\ln K$ as a function of the reciprocal temperature. The values of enthalpy and entropy obtained from Figure 1 are $\Delta H = 12.2$ kJ mol^{-1} and $\Delta S = 21.4$ J K^{-1} mol^{-1}, respectively.

Kinetic Analysis. The kinetic analysis was carried out by using a computer program based on the modified Bloch equation for the two-site exchange as described previously.[13,15]

Results

Structure of $UO_2(acac)_2Me_2SO$ in o-$C_6H_4Cl_2$ Solution Containing Free Hacac. In the previous paper,[13] we reported that the structure of $UO_2(acac)_2Me_2SO$ in CD_3COCD_3 and CD_2Cl_2 was pentagonal bipyramidal. In order to confirm the structure of $UO_2(acac)_2Me_2SO$ in o-$C_6H_4Cl_2$ solutions containing free Hacac, the NMR, UV, and IR spectra were measured in solution.

The ^1H NMR spectra are shown in Figure 2. Signals a and b correspond to the methyl protons of the enol and keto isomers of Hacac, respectively. The c and d signals are the methyl protons of the coordinated acac and Me_2SO, respectively. At 50 °C, the area ratios of signals a to b to c and of signals d to c show that two acac ions and one Me_2SO molecule coordinate to the uranyl ion. This fact suggests that the following equilibrium does not exist to any appreciable extent:

$$UO_2(acac)_2Me_2SO + Hacac \rightleftharpoons UO_2(acac)_2acacH + Me_2SO \quad (1)$$

In order to support the result of the ^1H NMR study, measurements of UV and IR spectra were carried out for two solutions, i.e. (1) the o-$C_6H_4Cl_2$ solution containing $UO_2(acac)_2Me_2SO$ and free Hacac and (2) the o-$C_6H_4Cl_2$ solution containing only $UO_2(acac)_2Me_2SO$. In the IR spectra, the S=O stretching of $UO_2(acac)_2Me_2SO$ in the former and the latter solutions was observed at 998 and 994 cm^{-1}, respectively, which are 57 and 61 cm^{-1} lower than the corresponding value in pure Me_2SO (1055 cm^{-1}). These results indicate that the Me_2SO molecule is coordinated to the uranyl ion through oxygen, because it has been reported[16] that the S=O stretching

(1) Ikeda, Y.; Soya, S.; Tomiyasu, H.; Fukutomi, H. *J. Inorg. Nucl. Chem.* **1979**, *41*, 1333.
(2) Ikeda, Y.; Tomiyasu, H.; Fukutomi, H. *Bull. Res. Lab. Nucl. React. (Tokyo Inst. Technol.)* **1979**, *4*, 47.
(3) Bowen, R. P.; Lincoln, S. F.; Williams, E. H. *Inorg. Chem.* **1976**, *15*, 2126.
(4) Crea, J.; Digiusto, R.; Lincoln, S. F.; Williams, E. H. *Inorg. Chem.* **1977**, *16*, 2825.
(5) Honan, G. J.; Lincoln, S. F.; Williams, E. H. *Inorg. Chem.* **1978**, *17*, 1855.
(6) Honan, G. J.; Lincoln, S. F.; Williams, E. H. *J. Chem. Soc., Dalton Trans.* **1979**, 320.
(7) Honan, G. J.; Lincoln, S. F.; Williams, E. H. *J. Chem. Soc., Dalton Trans.* **1979**, 1220.
(8) Bowen, R. P.; Honan, G. J.; Lincoln, S. F.; Spotswood, T. M.; Williams, E. H. *Inorg. Chim. Acta* **1979**, *33*, 2351.
(9) Honan, G. J.; Lincoln, S. F.; Williams, E. H. *Aust. J. Chem.* **1979**, *32*, 1851.
(10) Hounslow, A. M.; Lincoln, S. F.; Marshall, P. A.; Williams, E. H. *Aust. J. Chem.* **1981**, *34*, 2543.
(11) Vasilescu, A. *Rev. Roum. Chim.* **1975**, *20*, 951.
(12) Bokolo, K.; Delpuech, J.-J.; Rodehüser, L.; Rubini, P. R. *Inorg. Chem.* **1981**, *20*, 992.
(13) Ikeda, Y.; Tomiyasu, H.; Fukutomi, H. *Bull. Chem. Soc. Jpn.* **1983**, *56*, 1060.
(14) Ikeda, Y.; Tomiyasu, H.; Fukutomi, H. *Inorg. Chem.* **1984**, *23*, 1356.
(15) Binsch, G. *Top. Stereochem.* **1968**, *3*, 97.

0020-1669/84/1323-3197$01.50/0

Table I. Solution Compositions and Kinetic Parameters for the Exchange of acac in $UO_2(acac)_2Me_2SO$ in o-$C_6H_4Cl_2$

soln	$[UO_2(acac)_2Me_2SO]/10^{-2}$ M	[Hacac]/M	$[o\text{-}C_6H_4Cl_2]$/M	$\Delta H^{\ddagger}$/kJ mol^{-1}	$\Delta S^{\ddagger}$/J K^{-1} mol^{-1}	k_{ex}(80 °C)/s^{-1}
i	6.17	0.147	8.85	51.7 ± 0.8	−86.9 ± 2.5	5.35 ± 0.3
ii	6.00	0.256	8.71	53.3 ± 1.3	−77.3 ± 3.8	9.91 ± 1.3
iii	6.02	0.301	8.64	52.1 ± 1.3	−78.5 ± 2.9	12.2 ± 1.3
iv	6.28	0.580	8.56	55.9 ± 1.7	−63.8 ± 4.6	17.6 ± 0.8
v	6.04	0.605	8.52	52.9 ± 2.5	−72.7 ± 7.1	18.0 ± 1.1
vi	6.15	0.703	7.96	51.2 ± 1.7	−76.0 ± 5.0	21.5 ± 0.8
vii	1.56	0.300	8.84	48.3 ± 1.7	−88.8 ± 5.1	13.6 ± 1.9
viii	3.59	0.305	8.72	54.3 ± 1.3	−71.2 ± 3.2	14.4 ± 1.3

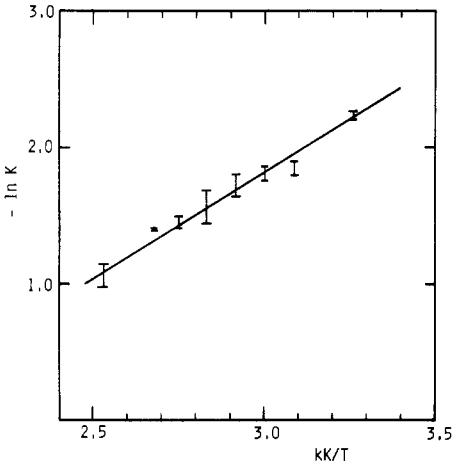

Figure 1. Plot of $-\ln K$ vs. $1/T$ for the keto–enol equilibrium of acetylacetone in o-$C_6H_4Cl_2$.

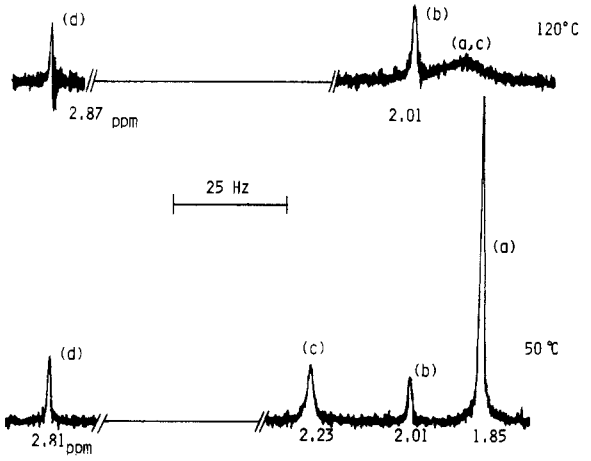

Figure 2. ^1H NMR spectra of a solution consisting of $UO_2(acac)_2Me_2SO$ (0.0679 M), Hacac (0.487 M), and o-$C_6H_4Cl_2$ (8.62 M) at 50 and 120 °C.

frequency decreases when the Me_2SO molecule coordinates through oxygen. Furthermore, the UV spectra of two solutions were self-consistent. From these results, it can be concluded that even if the free Hacac is present in solution, the equilibrium as shown in eq 1 does not exist to any measureable extent and the pentagonal-bipyramidal structure is maintained.

Exchange Reaction of acac in $UO_2(acac)_2Me_2SO$. It is apparent from Figure 2 that the keto isomer of Hacac does not exchange with the coordinated acac of $UO_2(acac)_2Me_2SO$ in this temperature region (50–120 °C). If the keto isomer exchanges with the coordinated acac, the chemical shift and line width of the keto methyl proton signal should be changed with increasing temperature. However, such a phenomenon was not observed. The methyl proton signal of the coordinated Me_2SO was observed at the same resonance frequency at 50 and 120 °C. The methyl proton signals of the coordinated acac and the free Hacac coalesce around 120 °C. These facts indicate that the following exchange occurs in the temperature range higher than 50 °C:

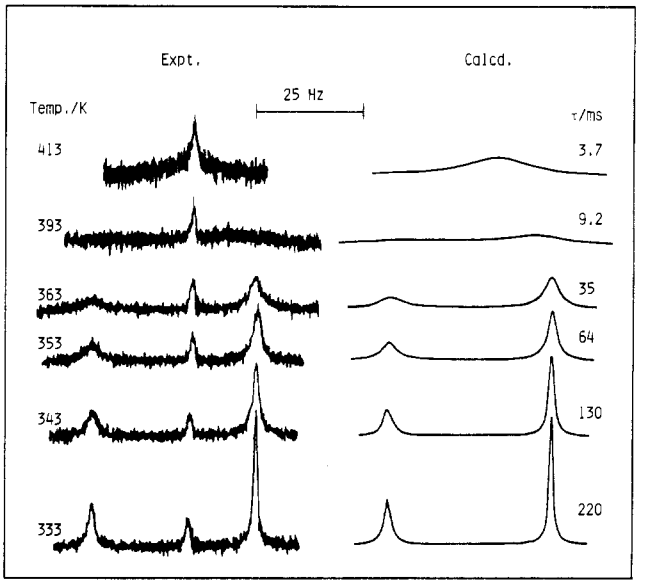

Figure 3. Experimental (left side) and best-fit calculated ^1H NMR line shapes of a solution consisting of $UO_2(acac)_2Me_2SO$ (0.0600 M), Hacac (0.256 M), and o-$C_6H_4Cl_2$ (8.71 M). Temperatures and best-fit τ values are shown on the left and right sides of the figure, respectively.

$$UO_2(acac)_2Me_2SO + enol^* \rightleftharpoons UO_2(acac)(acac^*)Me_2SO + enol \quad (2)$$

where the asterisk is used to denote the exchange species.

Figure 3 shows the line shapes for the methyl proton signal of the coordinated acac and the free Hacac as a function of temperature. The best-fit τ values at each temperature are shown at the right side of Figure 3 together with the corresponding calculated line shapes. The first-order rate constant, k_{ex}, was calculated from eq 3 and 4, where τ and P with the

$$\tau = \tau_c P_f = \tau_f P_c \quad (3)$$

$$k_{ex} = 1/\tau_c = (\text{rate})/2[UO_2(acac)_2Me_2SO] \quad (4)$$

subscripts of c and f are the mean lifetimes and the mole fractions of the coordinated and free sites, respectively.

The measurements of k_{ex} were carried out for the solutions listed in Table I. The logarithm of k_{ex} was plotted against the reciprocal temperature (Figure 4). It is observed from Figure 4 and Table I that k_{ex} increases with increasing [enol] (solutions i–vi) and is constant regardless of the change in the complex concentrations (solutions iii, vii, and viii). Plots of k_{ex} against [enol] are shown in Figure 5. This figure indicates that k_{ex} approaches a constant value as [enol] increases. Plots of $1/k_{ex}$ vs. $1/[enol]$ give straight lines with intercepts as shown in Figure 6 and hence yield the expression

$$1/k_{ex} = k_a + k_b[enol]^{-1} \quad (5)$$

(16) Cotton, F. A.; Francis, R. *J. Am. Chem. Soc.* **1960**, *82*, 2986.

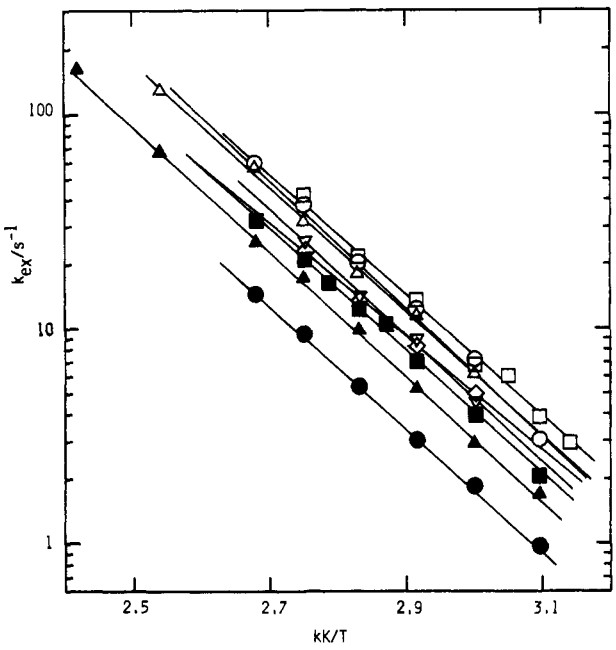

Figure 4. Semilogarithmic plots of k_{ex} vs. $1/T$ for the exchange of acac in $UO_2(acac)_2Me_2SO$. The symbols of ●, ▲, ■, ○, △, □, ◇, and ▽ correspond to solutions i, ii, iii, iv, v, vi, vii, and viii in Table I, respectively.

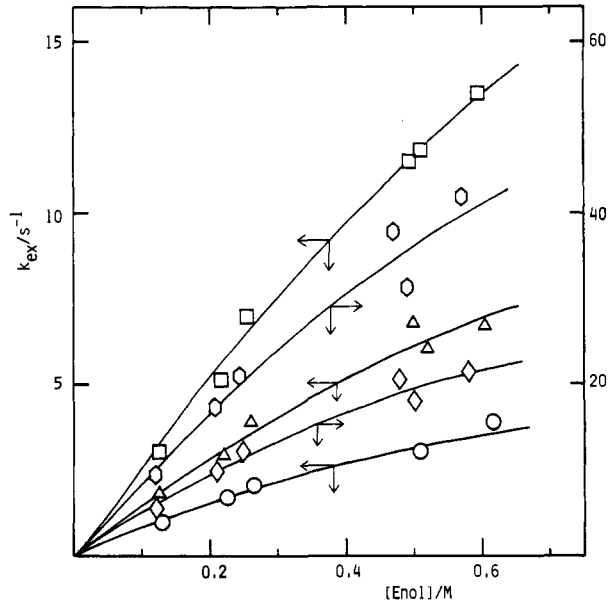

Figure 5. Plots of k_{ex} vs. [enol] for the exchange of acac in $UO_2(acac)_2Me_2SO$: (○) 50 °C; (△) 60 °C; (□) 70 °C; (◇) 80 °C; (○) 90 °C.

The values of k_a and k_b were obtained by means of the least-squares method from the intercepts and slopes in Figure 6, respectively. The results are listed in Table II.

Effect of Added Me_2SO on the Exchange Rate of acac. In a previous paper,[13] the Me_2SO exchange in $UO_2(acac)_2Me_2SO$ was studied by NMR. It was found that the Me_2SO exchange proceeds through the D and I mechanisms,[17] and the exchange rate constant is larger than 10^3 s^{-1} in the present temperature range (50–140 °C). In order to examine the effect of added Me_2SO on the acac exchange, experiments were carried out in solutions including free Me_2SO. The results are listed in Table III and Figure 7. Figure 7 shows that the exchange

(17) Langford, C. H.; Gray, H. B. "Ligand Substitution Processes"; Benjamin: London, 1974.

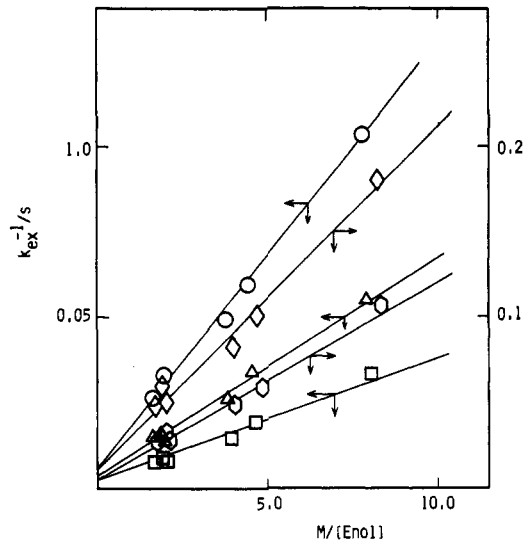

Figure 6. Plots of $1/k_{ex}$ vs. $1/[enol]$ for the exchange of acac in $UO_2(acac)_2Me_2SO$: (○) 50 °C; (△) 60 °C; (□) 70 °C[; (◇) 80 °C; (○) 90 °C.

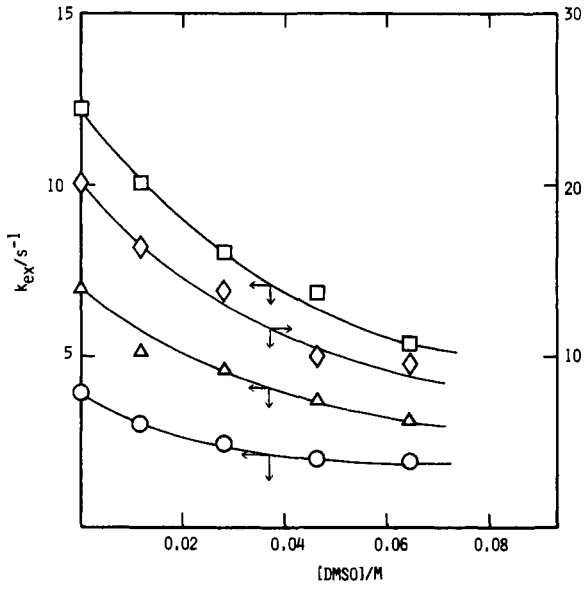

Figure 7. Plots of k_{ex} vs. $[Me_2SO]$ for the effect of added Me_2SO on the exchange of acac in $UO_2(acac)_2Me_2SO$: (○) 60 °C; (△) 70 °C; (□) 80 °C; (◇) 90 °C.

Table II. Values of k_a, k_b, k_1, k_I, k_2/k_{-1}, and K_{os} at Various Temperatures and Kinetic Parameters for the k_1 or k_I Pathway

temp/ °C	k_a/ 10^{-3} s	k_b/ 10^{-2} M s	k_1 or k_I/ 10 s^{-1}	k_2/k_{-1} or K_{os}/M^{-1}
50	59.5 ± 26.3	12.3 ± 0.6	1.68 ± 0.74	0.48 ± 0.21
60	24.5 ± 14.0	6.61 ± 0.03	3.92 ± 2.24	0.39 ± 0.22
70	11.7 ± 10.5	3.62 ± 0.02	8.58 ± 7.70	0.32 ± 0.29
80	6.83 ± 7.49	2.14 ± 0.02	14.6 ± 16.0	0.32 ± 0.35
90	3.27 ± 3.08	1.19 ± 0.07	30.6 ± 28.8	0.27 ± 0.25

k_1 or k_I (25 °C) = 2.04 s^{-1}, $\Delta H^{\ddagger}$ = 66.4 ± 8.4 kJ mol^{-1}, $\Delta S^{\ddagger}$ = −17.1 ± 26.8 J K^{-1} mol^{-1}

rate becomes slower as the concentration of added Me_2SO increases. The plots of $1/k_{ex}$ vs. $[Me_2SO]$ are linear with varying intercepts as shown in Figure 8. This relation is given by eq 6. The values of k_a' and k_b' were obtained by means

$$1/k_{ex} = k_a' + k_b'[Me_2SO] \quad (6)$$

of least-squares methods from the intercepts and slopes in Figure 8 and are listed in Table IV.

Table III. Solution Compositions and Kinetic Parameters for the Exchange of acac in $UO_2(acac)_2Me_2SO$ in o-$C_6H_4Cl_2$ Containing Free Me_2SO

soln	$[UO_2(acac)_2Me_2SO]$/ 10^{-2} M	[Hacac]/ M	$[Me_2SO]$/ 10^{-2} M	$[o\text{-}C_6H_4Cl_2]$/ M	$\Delta H^{\ddagger}$/ kJ mol^{-1}	$\Delta S^{\ddagger}$/ J K^{-1} mol^{-1}	k_{ex}(80 °C)/ s^{-1}
i	6.02	0.301	0.0	8.64	52.1 ± 1.3	−78.5 ± 2.9	12.2 ± 1.3
ii	5.97	0.314	1.15	8.56	54.4 ± 1.0	−74.3 ± 2.7	10.1 ± 0.6
iii	5.95	0.300	2.82	8.55	55.3 ± 0.8	−73.2 ± 2.2	8.01 ± 1.13
iv	5.88	0.304	4.61	8.50	53.6 ± 1.8	−80.0 ± 5.2	6.87 ± 0.56
v	5.84	0.299	6.40	8.46	52.6 ± 1.1	−83.6 ± 3.2	5.36 ± 0.37

Table IV. Values of k_a', k_b', k_3/k_2, and K_{os}' at Various Temperatures

temp/ °C	k_a'/ 10^{-2} s	k_b'/ M^{-1} s	k_3/k_2	K_{os}'/ M^{-1}
60	26.2 ± 0.6	5.13 ± 0.15	51.9	20.2
70	15.1 ± 0.7	2.57 ± 0.20	56.9	18.2
80	8.04 ± 0.39	1.58 ± 0.10	57.4	18.4
90	4.91 ± 0.28	0.902 ± 0.073	67.3	18.2

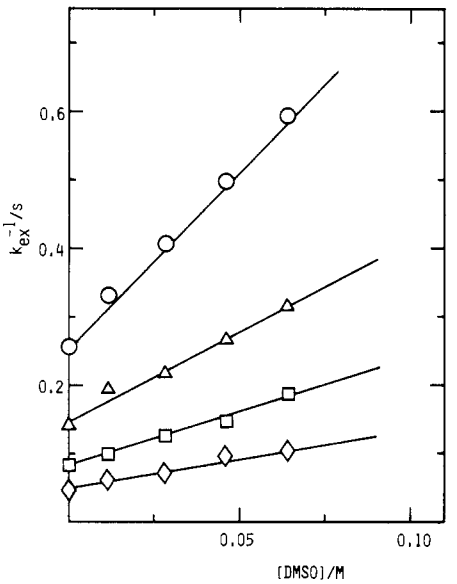

Figure 8. Plots of $1/k_{ex}$ vs. $[Me_2SO]$ for the effect of added Me_2SO on the exchange of acac in $UO_2(acac)_2Me_2SO$: (○) 60 °C; (△) 70 °C; (□) 80 °C; (◇) 90 °C.

Discussion

As is seen in Figure 5, the exchange rate increases as [enol] increases and approaches a constant value. From these results, two possible mechanisms are postulated for the acac exchange reaction as shown in Scheme I, i.e. mechanism 1 (I → II → IV → IV′ → I′) or mechanism 2 (I → III → IV → IV′ → I′). In mechanism 1, the rate-determining step is the pathway I → II. Intermediate II is a four-coordinated complex in the equatorial plane, in which one of two acac ions coordinates as a unidentate ligand. Intermediate IV is formed by coordination of the incoming enol isomer (Hacac*) to intermediate II. The proton transfer takes place in pathway IV → IV′, followed by ring closure of the unidentate acac*. When the steady-state approximation is applied to intermediate II, the first-order exchange rate constant, k_{ex}, is given by eq 7.

$$k_{ex} = \frac{k_1k_2[\text{enol}]}{k_{-1} + k_2[\text{enol}]} \tag{7a}$$

$$\frac{1}{k_{ex}} = \frac{1}{k_1} + \frac{k_{-1}}{k_1k_2[\text{enol}]} \tag{7b}$$

Equation 7b is consistent with eq 5. The rate constants in mechanism 1 are related to k_a and k_b in eq 5 as follows:

$$k_a = 1/k_1 \qquad k_b = k_{-1}/(k_1k_2) \tag{8}$$

Scheme I

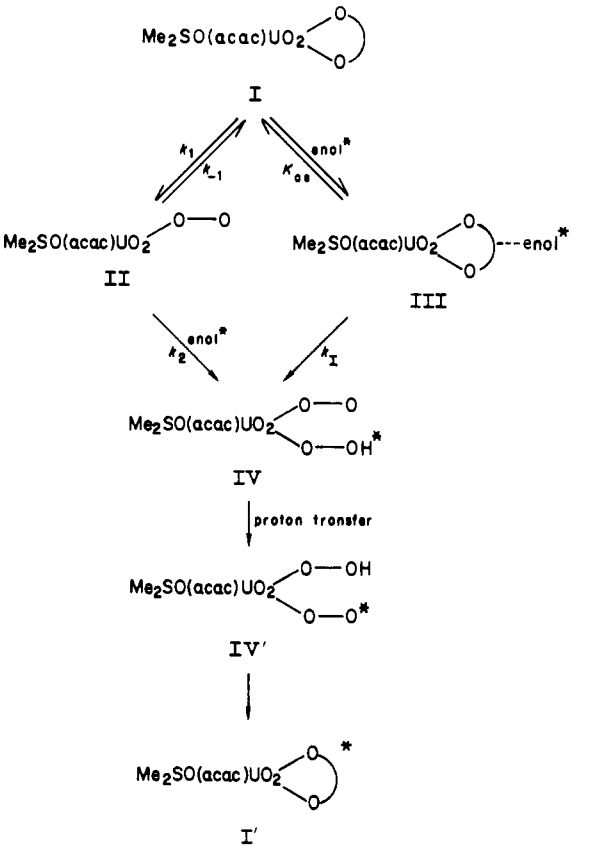

The values of k_1 and k_2/k_{-1} were obtained from k_a and k_b and are listed in Table II.

In mechanism 2, III is the outer-sphere complex and K_{os} is the outer-sphere complex formation constant. In the pathway III → IV, the dissociation of one end of the coordinated acac occurs, followed by the coordination of the incoming enol isomer, which is in the second-coordination sphere, and k_I is the rate constant for the corresponding pathway. In this mechanism, k_{ex} is given by eq 9. Equation 9b is also

$$k_{ex} = \frac{k_IK_{os}[\text{enol}]}{1 + K_{os}[\text{enol}]} \tag{9a}$$

$$\frac{1}{k_{ex}} = \frac{1}{k_I} + \frac{1}{k_IK_{os}[\text{enol}]} \tag{9b}$$

consistent with eq 5, and hence the kinetic parameters in mechanism 2 are related to k_a and k_b in eq 5 as follows:

$$k_a = 1/k_I \qquad k_b = 1/(k_IK_{os}) \tag{10}$$

Combination of eq 8 and 10 leads to the relations $k_1 = k_I$ and $k_2/k_{-1} = K_{os}$. The values of k_I and K_{os} are listed in Table II. The activation parameters for k_1 or k_I are also shown in Table II. The $\Delta S^{\ddagger}$ value has an only slightly negative value. This may be consistent with the view that pathway I → II or III → IV proceeds dissociatively.

Scheme II

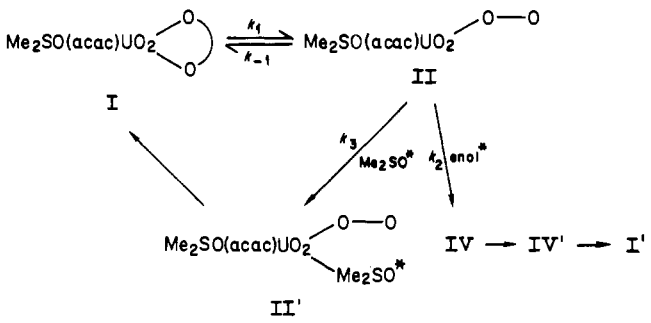

Scheme III

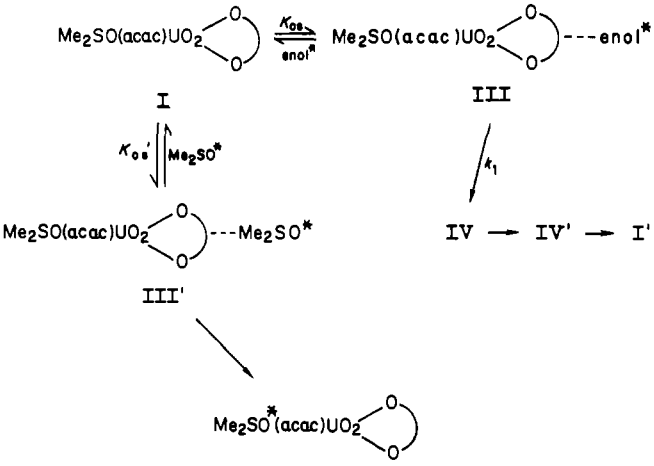

Extrapolation of the value of k_2/k_{-1} or K_{os} to 25 °C gives $k_2/k_{-1} = K_{os} = 0.89$ M^{-1}. This K_{os} value is nearly equal to that estimated from the Fuoss equation[18] for an interaction distance of 7 Å and is smaller than the corresponding value (4.9 ± 1.8 M^{-1}) for the Me_2SO exchange in $UO_2(acac)_2Me_2SO$ in CD_2Cl_2. This may be explained by considering that Gutmann's donor number (DN) of Hacac (DN = 20.0)[19] is smaller than that of Me_2SO (DN = 29.8).[20] On the other hand, it also seems to be reasonable that k_{-1} is larger than k_2, because k_{-1} is the rate constant for the chelation of unidentate acac. The reaction of uranyl ion with Hacac was studied,[21] and the formation rate constant of the mono(acetylacetonato) complex was reported to be 4.93×10^3 M^{-1} s^{-1} at 25 °C in methanol–water mixtures. If the value of k_2 is assumed to be equal to or less than 4.93×10^3 M^{-1} s^{-1}, the value of k_{-1} is estimated to be less than 5.6×10^3 s^{-1} at 25 °C. It is not unreasonable that k_{-1} is larger than the exchange rate constant of unidentate ligand in uranyl complexes. In fact, the rate constants of the Me_2SO exchange in $[UO_2(Me_2SO)_5]^{2+}$ and $UO_2(acac)_2Me_2SO$ are 5.53×10^3 s^{-1} and 2.36×10^2 s^{-1}, respectively.[2,13] Although it is difficult to determine which mechanism is more acceptable, it might be reasonable that the rate-determining step is the dissociation of one end of the coordinated acac and that the exchange reaction passes through intermediate IV.

As mentioned above, the exchange rate of acac becomes slower by the addition of free Me_2SO (Figure 7), but the $\Delta H^{\ddagger}$ value for the first-order rate constant in the presence of free Me_2SO is very similar to that in the absence of free Me_2SO (Table III). This fact suggests that the exchange reaction of acac proceeds through the same mechanism even in the presence of free Me_2SO. If the acac exchange reaction proceeds through mechanism 1 or 2 and Me_2SO competes with free Hacac to coordinate at the vacant site, mechanisms 1 and 2 are modified as shown in Schemes II and III, respectively.

In Scheme II, Me_2SO is shown to compete with free Hacac in the attack on the vacant site of intermediate II. On the other hand, in Scheme III, Me_2SO forms an outer-sphere complex with $UO_2(acac)_2Me_2SO$ in the pathway I → III'. This complex formation results in a decrease in the concentration of outer-sphere complex III and in the exchange rate. In Scheme II, k_{ex} is expressed by eq 11. The corresponding

$$k_{ex} = \frac{k_1k_2[\text{enol}]}{k_{-1} + k_2[\text{enol}] + k_3[Me_2SO]} \quad (11a)$$

$$\frac{1}{k_{ex}} = \frac{k_{-1} + k_2[\text{enol}]}{k_1k_2[\text{enol}]} + \frac{k_3[Me_2SO]}{k_1k_2[\text{enol}]} \quad (11b)$$

rate constant in Scheme III is given by eq 12. Under the

$$k_{ex} = \frac{k_1K_{os}[\text{enol}]}{1 + K_{os}[\text{enol}] + K_{os}'[Me_2SO]} \quad (12a)$$

$$\frac{1}{k_{ex}} = \frac{1 + K_{os}[\text{enol}]}{k_1K_{os}[\text{enol}]} + \frac{K_{os}'[Me_2SO]}{k_1K_{os}[\text{enol}]} \quad (12b)$$

present experimental conditions, [enol] is nearly constant as shown in Table III. It is apparent that eq 11b or 12b correlates with eq 6 at [enol] ≃ constant, where k_a' and k_b' in eq 6 correspond to the respective coefficients of eq 11b or 12b as follows. For eq 11b

$$k_a' = \frac{k_{-1} + k_2[\text{enol}]}{k_1k_2[\text{enol}]} \quad (13a)$$

$$k_b' = \frac{k_3}{k_1k_2[\text{enol}]} \quad (13b)$$

and for eq 12b

$$k_a' = \frac{1 + K_{os}[\text{enol}]}{k_1K_{os}[\text{enol}]} \quad (14a)$$

$$k_b' = \frac{K_{os}'}{k_1K_{os}[\text{enol}]} \quad (14b)$$

As the values of [enol], k_1, k_1, and K_{os} are already obtained as shown in Tables II and III, the values of k_3/k_2 and K_{os}' can be calculated from the value of k_b' in Table IV. The results are listed in Table IV. The values of k_3/k_2 and K_{os}' at 25 °C are estimated to be about 32 and 28 M^{-1}, respectively, from the values of k_b' (57 M^{-1} s^{-1}), k_1 (2.04 s^{-1}), k_1 (2.04 s^{-1}), and K_{os} (0.89 M^{-1}) at 25 °C. The estimated K_{os}' value is much larger than the values expected from the Fuoss equation and obtained from the Me_2SO exchange in $UO_2(acac)_2Me_2SO$ in CD_2Cl_2 (4.9 ± 1.8 M^{-1}).[13] It is expected that K_{os}' in o-$C_6H_4Cl_2$ is smaller than that in CD_2Cl_2 because the dielectric constant of o-$C_6H_4Cl_2$ (9.93) is larger than that of CH_2Cl_2 (8.93). On the other hand, it may be reasonable that the value of k_3 is larger than that of k_2. As noted earlier, if the k_2 value is assumed to be approximately 4.93×10^3 M^{-1} s^{-1} at 25 °C, the k_3 value is estimated to be about 1.6×10^5 M^{-1} s^{-1} at 25 °C from the values of $k_3/k_2 = 32$. The estimated k_3 value is found to be much larger than those of the Me_2SO exchange in $[UO_2(Me_2SO)_5]^{2+}$ and $UO_2(acac)_2Me_2SO$.[2,13] This is reasonable considering that the k_3 pathway is the coordination of Me_2SO to the vacant site of intermediate II and corresponds to the fast pathway in the Me_2SO exchange process as follows:

$$UO_2(acac)_2Me_2SO + Me_2SO^* \xrightarrow[\text{slow}]{} UO_2(acac)_2 + Me_2SO + Me_2SO^* \xrightarrow[\text{fast}]{} UO_2(acac)_2Me_2SO^* + Me_2SO \quad (15)$$

The fact that $k_3 > k_2$ may be also explained by the relatively

(18) Fuoss, R. M. *J. Am. Chem. Soc.* **1958**, *80*, 5059.
(19) Nishizawa, M.; Saito, K. *Bull. Chem. Soc. Jpn.* **1978**, *51*, 483.
(20) Gutmann, V.; Schmid, R. *Coord. Chem. Rev.* **1974**, *12*, 263.
(21) Hynes, M. J.; O'Regan, B. D. *J. Chem. Soc., Dalton Trans.* **1980**, 1502.

higher affinity of Me_2SO than that of Hacac for uranyl ion. Furthermore, the larger size of Hacac could make it more difficult for Hacac to approach into the inner sphere of the uranyl ion as compared with Me_2SO.

In conclusion, it is more likely that the acac exchange in $UO_2(acac)_2Me_2SO$ proceeds through mechanism 1 (I → II → IV → IV′ → I′), but mechanism 2 cannot be discarded, because the Me_2SO exchange in $UO_2(acac)_2Me_2SO$ in CD_2Cl_2 proceeds through the I mechanism.[17]

Vasilescu[11] studied the exchange of acac in $UO_2(acac)_2$ in acetonitrile and proposed that the acac exchange proceeds through both unimolecular and bimolecular processes. However, the rate constant for the unimolecular process decreases with increasing temperature. It is well-known that uranyl β-diketonato complexes form a binuclear complex, $[UO_2(\beta\text{-diketonato})_2]_2$, in the absence of adduct ligands.[22,23] The basic difficulty in Vasilescu's study might arise from the fact that the dimerization of $UO_2(acac)_2$ was not considered.

Acknowledgment. The authors thank Professor Gilbert Gordon of Miami University and Professor Thomas W. Swaddle of the University of Calgary for helpful discussions.

Registry No. acac, 123-54-6; $UO_2(acac)_2Me_2SO$, 71357-22-7.

(22) Comyns, A. E.; Gatehouse, B. M.; Wait, E. *J. Chem. Soc.* **1958**, 4655.
(23) Casellato, U.; Vidali, M.; Vigato, P. A. *Inorg. Chim. Acta* **1976**, *18*, 77.

Contribution from the Department of Chemistry, Virginia Commonwealth University, Richmond, Virginia 23284

Ligand Control of *cis*-Dioxomolybdenum(VI) Redox Chemistry: Kinetic and Activation Parameter Data for Oxygen Atom Transfer

JOSEPH TOPICH* and JAMES T. LYON, III

Received July 7, 1983

The oxygen atom transfer reactions for MoO_2(5-X-SSP) and MoO_2(5-X-SSE) (5-X-SSP^{2-} = 2-((5-X-salicylidene)amino)benzenethiolate; 5-X-SSE^{2-} = 2-((5-X-salicylidene)amino)ethanethiolate; X = Br, Cl, H, CH_3O) with $PEtPh_2$ were studied in detail between 30 and 60 °C. The applicable rate law is $-d[Mo^{VI}O_2L]/dt = k_1[Mo^{VI}O_2L][PEtPh_2]$. The specific rate constants span the range from 8.4×10^{-4} M^{-1} s^{-1} (X = CH_3O) to 19.6×10^{-4} M^{-1} s^{-1} (X = Br) for MoO_2(5-X-SSP) at 30 °C and from 21.4×10^{-4} M^{-1} s^{-1} (X = CH_3O) to 34.8×10^{-4} M^{-1} s^{-1} (X = Br) for MoO_2(5-X-SSE) at 60 °C. Only oxo-Mo(IV) complexes are observed as products of these reactions. A linear dependence is observed between log (k_{1X}/k_{1H}) and the Hammett σ_p parameter for the ligand X substituents for the two series MoO_2(5-X-SSP) (ρ = +0.75) and MoO_2(5-X-SSE) (ρ = +0.42). Activation parameter data were obtained for MoO_2(5-H-SSP) (E_a = 67.9 kJ/mol, ΔH^* = 65.2 kJ/mol, ΔS^* = -86.5 J/(mol K)) and MoO_2(5-H-SSE) (E_a = 72.0 kJ/mol, ΔH^* = 70.3 kJ/mol, ΔS^* = -82.6 J/(mol K)). There exists a correlation between E_{Pc} and the specific rate constants for MoO_2(5-X-SSP) and MoO_2(5-X-SSE).

Introduction

A number of redox enzymes are known to depend upon a molybdenum-containing cofactor for enzyme activity.[1,2] Recent EXAFS studies[3-6] have implicated sulfur and nitrogen or oxygen as ligand donor atoms in the coordination sphere of the molybdenum. In addition, EXAFS data also suggest that the oxidized forms of xanthine oxidase[3,5] and sulfite oxidase[4,5] contain the MoO_2^{2+} unit while the reduced forms of xanthine dehydrogenase and reduced sulfite oxidase contain a single terminal oxo ligand.[6] The current understanding of these enzymes indicates that the molybdenum cycles between the +6 and +4 oxidation states in their reactions with substrate and subsequent reactivation.[7] In examining the reactions carried out by xanthine, sulfite, and aldehyde oxidase and also nitrate reductase, one finds that the only difference between the substrate before and after the reaction is the addition or removal of an oxygen atom. The two-electron oxygen atom transfer reaction[8] may be relevant to the understanding of the reactions of molybdoenzymes, although other mechanisms are certainly possible.[9]

Coordination complexes of molybdenum in the higher oxidation states also contain the molybdenum oxo group. In particular, Mo(VI) complexes possess exclusively the *cis*-dioxomolybdenum moiety.[10] Attempts have been made to prepare molybdenum coordination complexes that can carry out oxygen atom transfer reactions. Mo(VI) complexes have been found to oxidize thiols,[11] hydrazine,[12] polyketones,[13] and tertiary phosphines.[8] The *cis*-dioxomolybdenum(VI) dialkyldithiocarbamates ($MoO_2(S_2CNR_2)_2$) have been extensively studied with regard to these reactions. Barral et al.[8] have reported on the oxidation of triphenylphosphine (PPh_3) by $MoO_2(S_2CNPr_2)_2$. For the reaction in *o*-dichlorobenzene they report a specific rate constant at 41 °C of 2.3 M^{-1} s^{-1}. McDonald and Schulman[14] have described an analytical procedure for the spectrophotometric determination of PPh_3

(1) Bray, R. C.; Swann, J. C. *Struct. Bonding (Berlin)* **1972**, *11*, 107-144.
(2) Bray, R. C. *Enzymes, 3rd Ed. 1970-1976* **1975**, *12*, 299-419.
(3) Tullius, T. D.; Kurtz, D. M., Jr.; Conradson, S. D.; Hodgson, K. O. *J. Am. Chem. Soc.* **1979**, *101*, 2776-2779.
(4) Cramer, S. P.; Gray, H. B.; Rajagopalan, K. V. *J. Am. Chem. Soc.* **1979**, *101*, 2772-2774.
(5) Berg, J. M.; Hodgson, K. O.; Cramer, S. P.; Corbin, J. L.; Elsberry, A.; Pariyadath, N.; Stiefel, E. I. *J. Am. Chem. Soc.* **1979**, *101*, 2774-2776.
(6) Cramer, S. P.; Wahl, R.; Rajagopalan, K. V. *J. Am. Chem. Soc.* **1981**, *103*, 7721-7727.
(7) Gutteridge, S.; Bray, R. C. *Chem. Uses Molybdenum Proc. Int. Conf., 3rd* **1979**, 275-279.
(8) Barral, R.; Bocard, C.; Seree de Roch, I.; Sajus, L. *Tetrahedron Lett.* **1972**, 1693-1696.
(9) Stiefel, E. I. *Proc. Natl. Acad. Sci. U.S.A.* **1973**, *70*, 988-992.
(10) Stiefel, E. I. *Prog. Inorg. Chem.* **1977**, *22*, 1-223 and references therein.
(11) Meriwether, L. S.; Marzluff, W. F.; Hodgson, W. G. *Nature (London)* **1966**, *212*, 465-467.
(12) Huang, T.; Spence, J. T. *J. Phys. Chem.* **1968**, *72*, 4198-4202, 4573-4577.
(13) Verchere, J.-F.; Fleury, M. B. *Bull. Soc. Chim. Fr.* **1972**, 2611-2617.
(14) McDonald, D. B.; Schulman, J. I. *Anal. Chem.* **1975**, *47*, 2023-2024.

0020-1669/84/1323-3202$01.50/0